X-ray Diffraction Studies of the Thick Filament in Permeabilized Myocardium from Rabbit

Sengen Xu,* Donald Martyn,† Jessica Zaman,* and Leepo C. Yu*
*National Institute of Arthritis, Musculoskeletal and Skin Diseases, National Institutes of Health, Department of Health and Human Services, Bethesda, Maryland; and †Department of Bioengineering, University of Washington, Seattle, Washington

ABSTRACT Low angle x-ray diffraction patterns from relaxed permeabilized rabbit cardiac trabeculae and psoas muscle fibers were compared. Temperature was varied from 25°C to 5°C at 200 mM and 50 mM ionic strengths (μ), respectively. Effects of temperature and μ on the intensities of the myosin layer lines (MLL), the equatorial intensity ratio $I_{1,1}/I_{1,0}$, and the spacing of the filament lattice are similar in both muscles. At 25°C, particularly at $\mu = 50$ mM, the x-ray patterns exhibited up to six orders of MLL and sharp meridional reflections, signifying that myosin heads (cross-bridges) are distributed in a well-ordered helical array. Decreasing temperature reduced MLL intensities but increased $I_{1,1}/I_{1,0}$. Decreases in the MLL intensities indicate increasing disorder in the distribution of cross-bridges on the thick filaments surface. In the skeletal muscle, order/disorder is directly correlated with the hydrolysis equilibrium of ATP by myosin, [M.ADP.P_i]/[M.ATP]. Similar effects of temperature on MLL and similar biochemical ATP hydrolysis pathway found in both types of muscles suggest that the order/disorder states of cardiac cross-bridges may well be correlated with the same biochemical and structural states. This implies that in relaxed cardiac muscle under physiological conditions, the unattached cross-bridges are largely in the M.ADP.P_i state and with the lowering of the temperature, the equilibrium is increasingly in favor of [M.ATP] and [A.M.ATP]. There appear to be some differences in the diffraction patterns from the two muscles, however. Mainly, in the cardiac muscle, the MLL are weaker, the $I_{1,1}/I_{1,0}$ ratio tends to be higher, and the lattice spacing D_{10}, larger. These differences are consistent with the idea that under a wide range of conditions, a greater fraction of cross-bridges is weakly bound to actin in the myocardium.

INTRODUCTION

The ultrastructures of the cardiac muscle cells are similar to those in skeletal muscle. The sarcomeres contain similar contractile proteins: the interdigitating thick and thin filaments form a hexagonal lattice, and the myosin heads (cross-bridges) are arranged in an approximately helical array on the thick filament surface (1). Biochemically, the cardiac actomyosin ATP hydrolysis cycle follows the same pathway with kinetics similar to those of the skeletal ATPase cycle (2).

One striking mechanical feature of cardiac muscle that differs from skeletal muscle is the steep force-length relation on the ''ascending limb'' (sarcomere length between 1.7 μm and 2.3 μm) and the pronounced length dependence of the Ca^{2+} sensitivity—i.e., the Frank-Starling law of the heart. Several experimental results are consistent with the idea that variations in the interfilament separation (lattice spacing) as a result of changes in sarcomere length modulate the actin-myosin interaction (3), although lattice spacing may not be the only factor (4).

There exists a vast literature characterizing structural, mechanical, and biochemical properties of the skeletal actomyosin interactions, whereas comparatively little is known about cardiac muscle. One approach to gain insight into cardiac muscle contraction is to compare various characteristics of the cross-bridges in the two types of muscle fibers. The purpose of this study is to use low angle x-ray diffraction to compare the structures of the thick filaments in relaxed cardiac and skeletal muscles under closely matched conditions known to alter cardiac contractility. In a relaxed muscle, interactions between actin and myosin are mostly limited to the low affinity states—the weak binding states—in the ATP hydrolysis cycle. The weak binding states are obligatory and required for isomerization or transition to force-generating, strongly bound cross-bridges (5). Characterizing the weak binding states would therefore have implications for understanding the mechanism of force generation.

Equatorial x-ray diffraction and mechanical stiffness measurements of relaxed cardiac muscle fibers showed that when myofilament lattice spacing decreased, the binding between actin and myosin increased (6). However, equatorial measurements did not provide information about the structural state of the cross-bridges beyond its radial position in the lattice. Two-dimensional x-ray diffraction from mammalian skeletal muscle reveals not only the physical distribution but also the biochemical state of myosins in the thick filaments. It was shown that the distribution of the cross-bridges on the mammalian skeletal thick filament surface was highly temperature dependent (7,8) and was correlated with myosin conformations and biochemical states (9,8). The thick filaments are helically ordered only at higher temperatures (>20°C) and become progressively more disordered as temperature is lowered. In MgATP-containing solutions, a well-ordered thick filament signifies that most of the myosins contain MgADP.P_i at their active site (10). In contrast, the myosin·ATP state is disordered, as is the analogous state myosin·AMPPNP (11).

Submitted May 25, 2006, and accepted for publication August 8, 2006.
Address reprint requests to Leepo C. Yu, E-mail: yule@mail.nih.gov.

0006-3495/06/11/3768/08 $2.00
doi: 10.1529/biophysj.106.088971

Matsubara and colleagues (12) pioneered two-dimensional x-ray diffraction studies from intact heart muscle. With the technology available at the time, information extracted from the studies was limited. In this study, two-dimensional x-ray diffraction patterns from relaxed permeabilized rabbit cardiac and psoas muscle fibers are compared at several temperatures and ionic strengths (μ). Similar temperature dependence found in the myosin layer line (MLL) intensities suggests that under physiological conditions, the cardiac cross-bridges are largely distributed in the M.ADP.P_i state, but M.ATP is increasingly favored as the temperature is lowered. In the cardiac muscle, MLL are considerably weaker, the $I_{1,1}/I_{1,0}$ ratio is generally higher, and the lattice spacing larger, compared to the skeletal muscle. The results are consistent with the idea that a greater fraction of the cardiac cross-bridges is weakly bound to actin, probably in the A·M·ATP state.

Preliminary results were presented at the 2006 Biophysical Society meeting (13).

METHODS

Specimen preparation

Permeabilized trabeculae from rabbit hearts were used for x-ray diffraction experiments. The whole heart was removed rapidly from the anesthetized New Zealand White rabbit (2–3 kg) and pumped several times in the skinning solution. After being placed in the fresh skinning solution for ~20 min, the heart was opened and placed in the skinning solution with 1% triton X-100 for ~30 min at 5°C. Subsequently, the trabeculae (~0.5 mm in diameter, ~6 mm in length) were dissected from the right ventricle, fixed at the two ends at resting length. The specimens were kept in the skinning solution at 5°C with 1% triton X-100 for 12 h and then were stored in the skinning solution without the detergent, ready for use. The specimens were used for experiments within 3 days. Sarcomere length was adjusted to 2.1–2.2 μm under laser light diffraction. For comparison, permeabilized single bundles of fibers from rabbit psoas major were used (for details, see Xu et al. (14)).

Solutions

The following solutions were used for the experiments. 1), Skinning solution contained (in mM) 5 KH_2PO_4, 5 MgAc, 5 EGTA, 3 Na_2ATP, 50 CrP, 5 NaN_3, 2 dithiothreitol (DTT), protease inhibitor cocktail from Sigma (St. Louis, MO; 100 μM [4-(2-aminoethyl)benzenesulfonyl fluoride hydrochloride] (AEBSF), 4 μM bestatin, 1.4 μM E-64, 2.2 μM leupeptin, 1.5 μM pepstatin A, 80 μM aprotinin), pH = 7.0. 2), Relaxing solution contained (in mM) 2 MgATP, 2 $MgCl_2$, 2 EGTA, 5 DTT, 10 imidazole, pH 7.0, μ = 27 mM. μ was adjusted by adding 10 mM creatine phosphate and varied potassium propionate for μ = 50 mM (low μ) or 200 mM (high μ). An ATP-backup system, ~109 unit/ml creatine kinase was added in the relaxing solution. 3), Rigor solution contained (in mM) 2.5 EGTA, 2.5 EDTA, 10 imidazole, 5 DTT, 150 potassium propionate, pH 7.0, μ = 170 mM. Before applying the rigor solution, the sample was always rinsed several times with a ''quick rinse'' solution containing (in mM) 5 EGTA, 15 EDTA, 20 imidazole, pH 7.0, μ = 70 mM (14).

During the entire course of the experiments, the solution in the chamber was continuously mixed by a push-pull syringe pump at the rate of ~0.5 ml/s to minimize any concentration gradient along the length of the muscle. To reduce radiation damage, the specimen chamber was moved up and down continuously for a range of 4 mm at a constant rate of 4 mm/s by a stepping motor (Aerotech, Pittsburgh, PA).

X-ray source, camera, and detector system

The experiments were performed at beamline X27C (Advanced Polymer PRT) at the National Synchrotron Light Source, Brookhaven National Laboratory, Upton, NY. The optics of X27C used a double-multilayer (silicon/tungsten) monochromator. A three-pinhole system was used for collimating the monochromatized beam. The beam size at the specimen was ~0.4 mm in diameter and specimen-to-detector distance was 1500 mm. A MAR Research CCD detector (Hamburg, Germany) with 0.08 × 0.08 mm pixel size was used for collecting the x-ray data.

The sample was held vertical. The exposure time for each pattern was 2 min in general. The maximum accumulated exposure time for each muscle sample was ≤12 min. In some cases, the solution background patterns were taken at the end of a series of x-ray exposures on the sample.

To directly compare the intensities while minimizing random errors (e.g., muscle size and beam quality), a stringent experimental protocol was followed. Only experiments where diffraction patterns were obtained for a complete set of conditions were selected for this work. In general, six exposures were taken for each experiment in the following sequence: i), in relaxing solution μ = 200 mM (or 50 mM) at 5°C; ii), 25°C; iii), μ = 50 mM (or 200 mM) at 25°C; iv), 5°C; v), in rigor condition μ = 170 mM at 5°C; and vi), 25°C. The spacings of all reflections were calibrated at the beginning of this series of experiments by the 1/144.3 $Å^{-1}$ meridional reflection from skinned rabbit psoas muscle in rigor at μ = 170 mM and T = 25°C (see Xu et al. (14) for details).

In summary, the experimental protocol included stirring the chamber to avoid solution gradient, scanning the fibers through the beam to minimize local radiation damage, and comparing multiple experimental conditions from the same sample to ensure the reproducibility of the recorded data.

Data reduction and analysis

The data were displayed and analyzed on a Silicon Graphics Indigo workstation (Mountain View, CA). The data in the four quadrants were first rotated, folded, and averaged. The program made slices parallel to the meridian and slices parallel to the equator of the diffraction patterns. Intensities within each slice were integrated to generate one-dimensional intensity profiles for further analysis. All integrated intensities (I) in Table 1 were normalized by the integrated intensity of the first MLL (I_{MLL1}) obtained from the muscles in the relaxing solution at μ = 50 mM and 25°C.

TABLE 1 Changes in the first MLL intensity (ΔI_{MLL1}) as a function of temperature and ionic strength

Muscle type	Conditions,relaxed at= (mM)	T (°C)	ΔI^*_{MLL1}	mean ± SE	n
Trabeculae	200	5	0	N.A.	3
	200	25	0.52	0.03	3
	50	5	0.27	0.02	3
	50	25	1	N.A.	3
Psoas	200	5	0	N.A.	3
	200	25	0.60	0.06	3
	50	5	0.37	0.04	3
	50	25	1	N.A.	3

The pattern obtained from each individual relaxed muscle preparation at μ = 200 mM and T = 5°C was used as a background and was first subtracted from patterns obtained from the same bundle under the other conditions. The difference was then normalized (ΔI^*_{MLL1}) by the difference obtained for μ = 50 mM and T = 25°C so that the results obtained from different fiber bundles can be compared. With the subtraction and normalization, $\Delta I^*_{MLL1} = 0$ at μ = 200 mM and 5°C and $\Delta I^*_{MLL1} = 1$ at μ = 50 mM and 25°C. Three bundles from each type of muscle were used.

The horizontal slices along the equator were made with the width adjusted to cover the whole [1,0], [1,1] reflections. Two vertical slices on the meridian were made with widths of 0.002563 $Å^{-1}$ (wide slice), which covers whole M3 intensity, and 0.007527 $Å^{-1}$ (narrow slice), which only covers the central part of M3 to emphasize the M3 spacing changes. The vertical off-meridional slices parallel to the meridian were made with the ranges of 0.002377–0.006997 $Å^{-1}$ (422–143 Å in real space), which covers the whole main peak of the first MLL (see Fig. 1). Within the slices, the background was first subtracted using the PCA program (Nucleus, Oak Ridge, TN) by linear interpolation in the region of maxima (14). Intensities above the background were then integrated.

RESULTS

The two-dimensional x-ray diffraction patterns from permeabilized cardiac trabeculae muscle are generally rather weak and noisy compared to those from skinned rabbit psoas muscle. The success rate in obtaining clear diffraction patterns is also much lower. However, up to six orders of the MLL are generally visible from the relaxed trabeculae (Fig. 1, *A*, *B*, *D*, and *E*), whereas the actin layer lines are too weak to be detected. In the rigor state (Fig. 1 *C*), the first and the sixth actin layer lines become prominent, as expected. In addition, in the rigor pattern some weak lattice labeling on the first actin layer line is detectable (Fig. 1 *C*), indicating some degree of three-dimensional actin filament alignment.

Effects of temperature on layer lines

In general, the diffraction patterns from the relaxed cardiac muscle are affected by factors such as temperature and μ, similar to those from relaxed skeletal muscle. Temperature, in particular, has a strong effect on the intensity of the MLL. Fig. 1 shows typical diffraction patterns from a single trabeculae at 25°C and 5°C when μ was either 200 mM (Fig. 1, *A* and *B*) or 50 mM (Fig. 1, *D* and *E*). A total of three complete sets of data similar to Fig. 1 from three separate preparations was obtained. For technical reasons (different camera lengths), the diffraction patterns could not be combined into one for display.

The pattern (Fig. 1 *A*) at 25°C and $\mu = 200$ mM shows visible MLL, indicating a certain degree of helical order in the arrangement of the cross-bridges in the thick filament. In contrast at 5°C the layer lines are practically undetectable (Fig. 1 *B*), indicating that the helical array of the cross-bridges becomes highly disordered. Myosin-related reflections, particularly the first MLL and the third meridional reflections, are clearly stronger at the higher temperature.

When μ is lowered to 50 mM, the layer lines are stronger. A similar effect of temperature on the MLL and the meridional reflections is found, as shown in Fig. 1, *D* and *E*. The pattern shown in Fig. 1 *F* is the difference between Fig. 1, *D* and *E*. It emphasizes the increase in layer line intensities with higher temperature.

Integrated off-meridional intensity profiles: comparison to skeletal muscle

Fig. 2 displays the intensity profiles of vertical slices taken between 0.002377 and 0.006997 $Å^{-1}$ (between the *dotted lines* shown in Fig. 1, *A* and *C*) from Fig. 1, *A–E*. The width between the dotted lines covers most of the first MLL and the first actin layer line of the diffraction patterns. At $\mu = 200$ mM, decreasing the temperature from 25°C to 5°C causes nearly complete loss of the first MLL (Fig. 2 *A*). At low μ, the first MLL is evident at both temperatures (Fig. 2 *A*). For

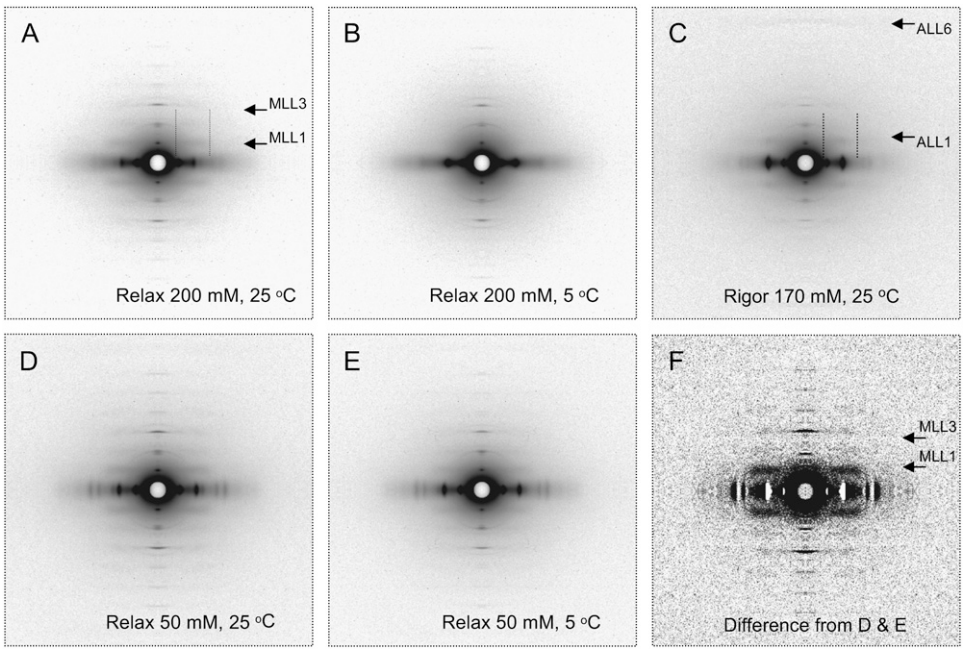

FIGURE 1 X-ray diffraction patterns from one rabbit trabeculae. Sarcomere length was 2.1 μm. In relaxing solution: (*A*) $\mu = 200$ mM and $T = 25$°C; (*B*) $\mu = 200$ mM and $T = 5$°C; (*D*) $\mu = 50$ mM and $T = 25$°C; (*E*) $\mu = 50$ mM at $T = 5$°C; in rigor solution: (*C*) $\mu = 170$ mM and $T = 25$°C. (*F*) A difference pattern obtained by subtracting pattern (*E*) from (*D*), emphasizing the increased intensities of the MLL, particularly the first layer line. Darkness indicates increase in intensity. Exposure time for each pattern was 2 min. The dotted lines in patterns (*A* and *C*) indicate the range of vertical slices made to obtain the intensity profiles of the layer lines shown in Fig. 2.

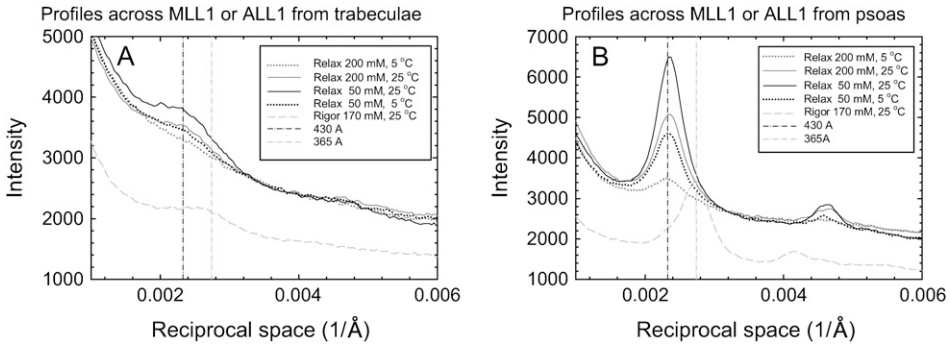

FIGURE 2 (*A*) Intensity profiles of vertical slices taken between 0.002377 and 0.006997 $Å^{-1}$ (between the *dotted lines* shown in Fig. 1 *A*) from Fig. 1, *A–E*. (*B*) Intensity profiles from a psoas fiber bundle under the same conditions (diffraction patterns not shown). In the relaxed muscle the MLL at 430 Å dominates the diffraction patterns, whereas in the rigor state the actin layer line at 365 Å dominates. The curves were shifted vertically to match the background levels to better demonstrate the intensity changes.

comparison, the much stronger intensity profiles from skinned rabbit psoas fibers obtained under identical conditions are shown in Fig. 2 *B*. For both muscles, the MLL are indexed on 430 Å and there is little density located at the first actin layer line (365 Å). In rigor, the MLL from both preparations become undetectable, whereas the actin layer line at 365 Å becomes predominant (Fig. 2). Changes in the layer line intensities are similar in that with increasing temperature, the intensity of the first MLL increases. Effects of ionic strength are also similar (see below).

Changes in the first MLL intensity as a function of temperature and ionic strength are summarized in Table 1 (three fiber bundles used). Intensity of the first MLL (I_{MLL1}) at 200 mM and 5°C, with few or no detectable layer lines, was taken as the baseline. It was subtracted from I_{MLL1} obtained under other conditions. Although the range of the variance is large, the combined data reinforce the observation in Fig. 1 that layer line intensities in both skeletal and cardiac muscle are strengthened by increasing temperature and lowered ionic strength.

Effects of ionic strength on layer line intensities

Ionic strength also affects the helical order of the myosin filament. By comparing the diffraction patterns at the same temperature (either at 25°C or 5°C) (Fig. 1, *A* and *D*, or Fig. 1, *B* and *E*, respectively) it is evident that raising μ decreases the layer line intensities. Similar effects have been found in rabbit psoas muscle (14). The changes cannot be attributed to myosin interaction with thin filaments, since in skeletal muscle, similar order-disorder transformation occurs when there is no actin-myosin overlap (10). The mechanism of the order-disorder effect will be addressed in Discussion.

Equatorial intensities

The equatorial intensities generally agree with our previous results from rat cardiac trabeculae and skinned rabbit psoas muscle: lowering temperature increases the $I_{1,1}/I_{1,0}$ ratio, indicating enhanced weak cross-bridge binding in both muscles (6,14). In Fig. 3 equatorial patterns obtained from cardiac trabeculae based on Fig. 1 (Fig. 3, *A*, *C*, and *E*) are compared to patterns from skinned skeletal fibers (Fig. 3, *B*, *D*, and *F*). The ratio of intensities of the [1,1] and [1,0] reflections ($I_{1,1}/I_{1,0}$) and the lattice spacing ($D_{1,0}$) from three separate bundles are summarized in Table 2.

As shown in Table 2, at $\mu = 200$ mM, lowering temperature from 25°C to 5°C increases the $I_{1,1}$ intensity and the intensity ratio (I_{11}/I_{10}) in both cardiac and skeletal fibers. At $\mu = 50$ mM, lowering the temperature also increases $I_{1,1}/I_{1,0}$ for both muscles. At the lower μ, the relative effect of temperature on the equatorial intensity ratio is diminished in both preparations: from 25°C to 5°C, at $\mu = 200$ mM the equatorial ratio is increased approximately threefold in cardiac and approximately twofold in skeletal fibers, whereas the corresponding changes at $\mu = 50$ mM are approximately twofold and ~1.5-fold, respectively (Table 2).

Myofilament lattice spacing ($D_{1,0}$) is influenced similarly by temperature and μ in both preparations. Lowering μ decreases $D_{1,0}$, whereas at each μ lowering temperature increases $D_{1,0}$ (Table 2). The changes in equatorial intensities with temperature and μ can be compared to the maximal changes observed in rigor for the cardiac (Fig. 3 *E*) and the skeletal (Fig. 3 *F*) bundles. As expected, the $I_{1,1}/I_{1,0}$ ratio increases significantly in rigor.

Meridional reflections

The intensities and spacings of the third myosin based meridional reflections (M3) from a trabecula are shown in Fig. 4 *A* and from psoas fibers in Fig. 4 *B*. In the relaxed state, M3 intensity increased with increasing temperature at both ionic strengths in skeletal fibers (Fig. 4 *B*). In cardiac muscle, M3 intensity increased at elevated temperature when $\mu = 50$ mm but was unchanged when $\mu = 200$ mM. The M3 spacing was 143.4 Å at 25°C for $\mu = 200$ mM and 50 mM in both preparations. At 5°C, the spacings of M3 diverged depending on μ and muscle. For the trabeculae, at $\mu = 50$ mM, it remained at 143.4 Å, whereas at $\mu = 200$ mM it shifted to 145.1 Å. For the psoas at $\mu = 200$ mM, one peak appeared at 147.6 Å and a small peak remained at 143 Å (Fig. 4 *B*). The rigor spacing in panels *A* and *B* was 144.3 Å and was used as calibration for all the measured spacings. The results indicate that, in general, changes in temperature and μ have similar

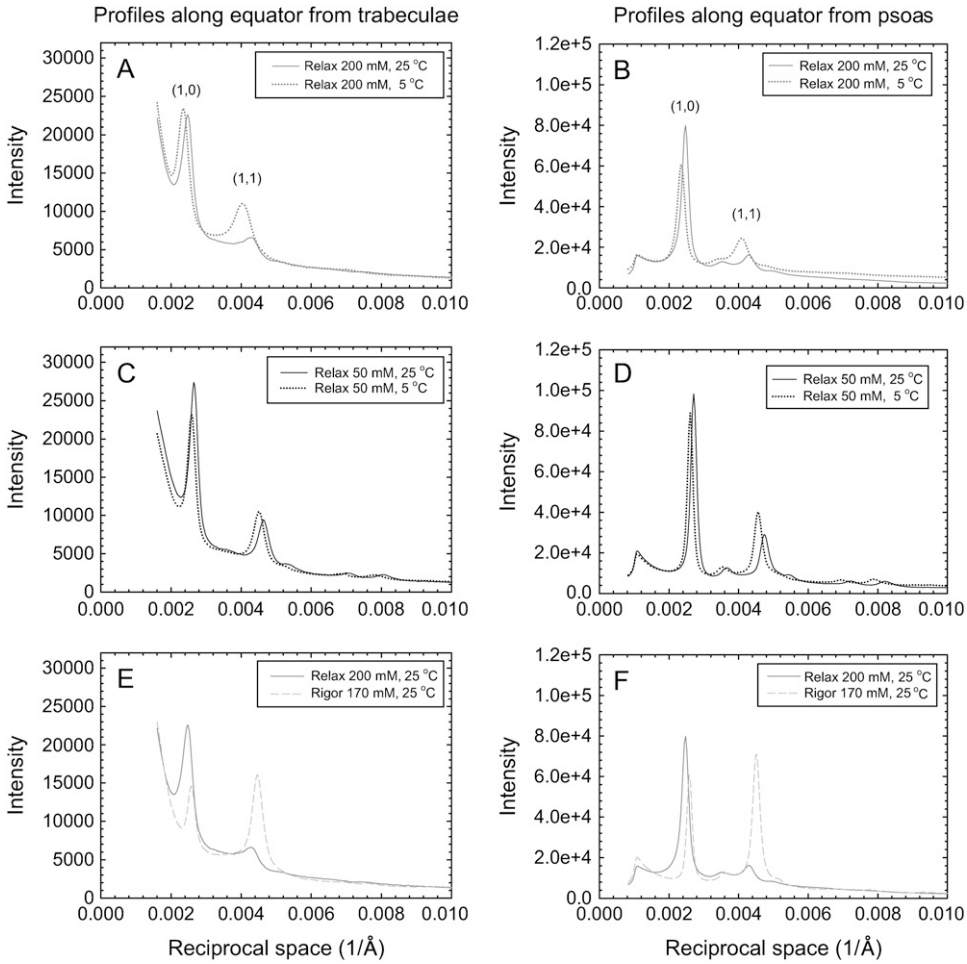

FIGURE 3 Equatorial intensity profiles: (*A*) from the trabaculae shown in Fig. 1, *A* and *B*, $\mu = 200$ mM at $T = 25°C$ and $T = 5°C$; (*B*): from a psoas bundle under the same conditions as (*A*); (*C*) From Fig. 1, *D* and *E*, with $\mu = 50$ mM at $T = 25°C$ and 5°C; (*D*) a psoas fiber bundle in relaxing solution with $\mu = 50$ mM at $T = 25°C$ and 5°C; (*E*) a trabeculae in relaxing solution with $\mu = 200$ mM and in rigor with $\mu = 170$ mM at $T = 25°C$; (*F*) a psoas fiber bundle in relaxing solution with $\mu = 200$ mM and in rigor with $\mu = 170$ mM at $T = 25°C$.

effects on the M3 reflections from cardiac and skeletal muscles.

DISCUSSION

Interpretation of the x-ray diffraction patterns from cardiac muscle as a function of temperature

The similarity between the cardiac and the skeletal results allows interpretation beyond the ordered or disordered arrangements of the myosin heads in the cardiac thick filaments. It has been shown previously that in a relaxed mammalian skeletal myosin filament the equilibrium between ordered ↔ disordered arrays of the myosin heads is strongly correlated with the equilibrium between the [M.ADP.P_i] and [M.ATP] states (15,10,8). An ordered array signifies an equilibrium in favor of the [M.ADP.P_i] population whereas a disordered array, the [M.ATP] population.

Although there is no direct correlation between filament structure and solution biochemistry for the cardiac muscle, the results obtained for skeletal myosin are applicable to cardiac myosin. The key characteristics of the diffraction patterns (e.g., the layer line intensities (Table 1), equatorial intensity ratio (Table 2), and the meridional reflections (Fig. 4)) show similar dependence on temperature. Furthermore, ATP hydrolysis by (porcine) cardiac S1 follows the same pathways as skeletal S1 with similar kinetics (2). Therefore, the order/disorder equilibrium in a relaxed cardiac muscle should also closely reflect the [M.ADP.P_i]/[M.ATP] equilibrium. It follows that at physiological temperatures large fractions of the cross-bridges in the cardiac muscle are

TABLE 2 Comparison of $D_{1,0}$ and $I_{1,1}/I_{1,0}$ from relaxed trabeculae and psoas muscle fiber bundles

Muscle type	Conditionsrelaxed at μ = (mM)	Temperature (°C)	$D_{1,0}$ ± (mean ± SE) ($n = 3$)(Å)	$I_{1,1}/I_{1,0}$ ± (mean ± SE) ($n = 3$)
Trabeculae	200	5	430 ± 5	0.89 ± 0.14
	200	25	414 ± 6	0.33 ± 0.12
	50	5	396 ± 7	1.19 ± 0.33
	50	25	381 ± 5	0.53 ± 0.11
Psoas	200	5	413 ± 9	0.47 ± 0.05
	200	25	395 ± 6	0.26 ± 0.03
	50	5	385 ± 3	0.68 ± 0.11
	50	25	372 ± 4	0.41 ± 0.04

Three muscle bundles were used.

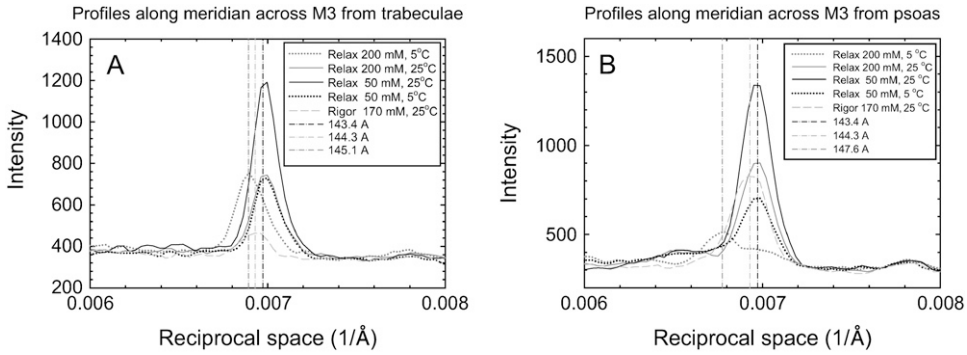

FIGURE 4 Intensity profiles along the meridian surrounding the third meridional reflection M3: (*A*) from a trabeculae, compared with (*B*) from a psoas fiber bundle under the same conditions.

expected to be in the [M.ADP.Pi] state. As temperature is lowered, [M.ATP] and [A.M.ATP] states are increasingly favored. To derive quantitative equilibrium constants for order/disorder and [M.ADP.P_i]/[M.ATP] at a given temperature, however, requires further experiments.

Ionic strength effects are distinct from the temperature effects

Evidence suggests that disorder by μ has an origin different from temperature. In solution, higher μ promotes hydrolysis of ATP by myosin S1 (16). One might expect improved helical order in the myosin filament as μ is raised, but the opposite has been observed (Figs. 1–3). Increasing μ significantly decreases, rather than increases, the intensities of the MLL (Fig. 1; (14)). At very high μ the myosin filament is dissolved. These results lead to the conclusion that increasing ionic strength has a predominant effect on disrupting the stability of the entire myosin filament, and its effect cannot be correlated with the biochemical states of the myosin heads.

The results in Table 2 suggest some differences in the equatorial diffraction patterns from the two muscles: the $I_{1,1}/I_{1,0}$ ratio is generally higher and the lattice spacing D_{10} is larger in the cardiac muscle. Since diffraction patterns were obtained under identical conditions, it is reasonable to make direct quantitative comparisons between the cardiac and skeletal results. Every mean value of $I_{1,1}/I_{1,0}$ listed in Table 2 from cardiac muscle appears to be higher, with some as high as doubling that of the skeletal data (at $\mu = 50$ mM and 5°C), although some of the differences in I_{11}/I_{10} are marginally significant and the variance of the cardiac data is greater than from skeletal fibers. Nevertheless, the current data point to a trend for a higher $I_{1,1}/I_{1,0}$ in cardiac muscle.

The higher $I_{1,1}/I_{1,0}$ for cardiac muscle suggests higher affinity between actin and myosin. Increases in $I_{1,1}/I_{1,0}$ in relaxed cardiac trabeculae were correlated with increased weak cross-bridge binding, as suggested by measurements of chord stiffness (6). Higher affinity has also been observed in solution. K_{app} for activation of actomyosin ATP hydrolysis is significantly lower for cardiac than for skeletal thin filament (H. White, Eastern Virginia Medical School, 2006, personal communication). In electron microscopic studies, it has been observed that interactions between the isolated thick and thin filaments under relaxing conditions appear to be more frequent for cardiac than for skeletal filaments (17,1).

The more abundant weakly bound cross-bridges could be populated in the A.M.ATP state, since the difference in $I_{1,1}/I_{1,0}$ is more prominent ($P = 0.05$) at low temperature and $\mu = 200$ mM (Table 2), where [M.ATP] and [A.M.ATP] are favored. The larger D_{10} spacing is also consistent with a larger fraction of cross-bridges attached in the [A.M.ATP] state (14). Furthermore, the M.ATP state is disordered on the thick filament, and the A.M.ATP attached state only gives rise to faint myosin and actin layer lines (11,14). This could be one of the causes for the weak MLL in the cardiac muscle, although fiber branching could also be an explanation (17,1).

One of the explanations for greater weak cross-bridge binding in cardiac muscle could be that weak binding is favored by a greater proportion of thin filament cross-bridge-binding sites in the ''closed'' state, as compared to skeletal thin filaments without Ca^{2+} (for reviews, see Gordon et al. (18) and Lehrer and Geeves (19)). Biochemical studies have indicated that the equilibrium distribution of skeletal and cardiac thin filaments between the ''blocked'' and ''closed'' states in the absence of Ca^{2+} may differ (20). Measurement of myosin S1 subfragment binding to thin filaments that were either regulated by skeletal or cardiac TnC complexed with skeletal TnI and TnT indicated that the fraction of thin filament sites in the ''closed'' state (permissive to weak cross-bridge binding) was greater with cardiac TnC than for the skeletal isoform in the absence of Ca^2 (20). If this comparison is valid for thin filaments reconstituted with skeletal Tn versus cardiac Tn, the increased equatorial intensity ratio for cardiac muscle (Table 1) could, at least in part, result from the increased availability of cardiac thin filament sites in the ''closed'' state for weak cross-bridge-thin filament interaction. Determination of the M.ATP ↔ M.ADP.Pi equilibrium for cardiac myosin and determination of the equilibrium distribution of cardiac thin filaments constituted with all cardiac regulatory protein isoforms will be needed to clarify the observed differences.

The order-disorder transition in the thick filaments may reflect changes in the flexibility of the myosin heads: physiological relevance of helical order and disorder

In the crystal structure of myosin S1 containing Mg.ADP.AlF_4 at its active site, the switch-II loop is ''closed'', whereas those containing Mg.ATP, the switch-II is ''open'' (for review, see Holmes and Geeves (21)). S1.ADP.AlF_4 is a close analog of the S1.ADP.P_i. S1 in the switch-II closed conformation is a stable and tightly packed structure, whereas in the switch-II open conformation the various domains are ''internally uncoupled'' with increased interdomain flexibility (22,23). A stable and less flexible S1 structure should result in decreased spatial fluctuations on the surface of the thick filament, revealing a well-ordered helical structure of the filament which gives rise to strong MLL. Conversely, an S1 with uncoupled internal domains would lead to a disordered filament and decreased layer line intensity.

A well-ordered filament consisting of rather inflexible myosin heads in the M.ADP.P_i state might appear somewhat paradoxical in view of the fact that maximal Ca^{2+}-activated force in skinned cardiac trabeculae increases with increasing temperature (24,25). In skinned rabbit psoas muscle at 25°C the myosin heads are arranged close to the surface of the thick filament (the center of mass of cross-bridges is at 135 Å from the center of the myosin filament) (7). Although precise measurement for the cardiac thick filament is not yet available, the center of mass of cardiac cross-bridges appears to be similarly located. Increased temperature favors cross-bridge proximity to the thick filament surface with apparently decreased cross-bridge mobility. In contracting muscle, where the attachment of the weak-binding M.ADP.Pi intermediate to the thin filaments is a critical step in the cross-bridge cycle (26), sequestering of the head away from the thin filament would be expected to reduce the rate of this reaction.

Several factors may resolve these apparent inconsistencies. Even in the ordered state, the heads are by no means completely rigid but show a degree of thermal/spatial disorder. In the model of Malinchik et al. (7) for skeletal muscle, for the ''ordered'' state the root mean square isotropic displacement was ~20 Å, making the thin filament within reach. Second, at physiological temperature the myosin heads are mostly in the prepower stroke, M.ADP.Pi state, poised to generate force. With increased rates of the ATP hydrolysis cycle at higher temperatures, the well-ordered filament structure should present no hindrance for generating higher force levels.

The disordered state of the thick filament may increase the proximity of the myosin heads to the thin filament and enhance the probability of cross-bridge-thin filament interaction. Phosphorylation of the regulatory light chain in skeletal muscle disorders myosin heads in isolated thick filaments (27), increases force calcium sensitivity (24,28), and increases the tension redevelopment rate at submaximal Ca^{2+} activation (29,30). Sweeney et al. (31) suggested that the enhancement of submaximal force and tension redevelopment kinetics could be due to closer proximity of the disordered myosin heads to thin filaments. In skinned cardiac trabeculae, regulatory light chain phosphorylation increased both maximal force and Ca^{2+} sensitivity and increased force redevelopment kinetics at submaximal [Ca^{2+}] (32). It could be that some flexibility is introduced into the rather inflexible M.ADP.P_i state by phosphorylation, and the number of cross-bridges bound to actin thus increases. Further x-ray diffraction experiments plus mechanical measurements are needed to test these ideas.

Implications for understanding cardiac function—the Frank-Starling relation

There is significant evidence that the steep enhancement of force with increasing sarcomere length in cardiac muscle results from increased cross-bridge proximity to thin filament binding sites (33,34), although there is evidence that lattice spacing may not be the only factor (4). It should be noted that the steep length dependence of force is maintained only at higher temperatures, whereas lowering temperature eliminates the effects of sarcomere length on force at all activating [Ca^{2+}] (24). The recent suggestions that cross-bridge affinity for actin in the weak-binding states (M.ATP and M.ADP.P_i) is modulated by lattice spacing offers a potential explanation for the strong temperature dependence of length-dependent activation (6,33,34). At low temperature, where the M.ATP state is favored, a significant fraction of the cross-bridges, with their flexible structures, may have ready access to binding sites on the thin filament. Under these conditions the influence of the lattice spacing on cross-bridge-thin filament interaction may be rendered less crucial to force generation. Increasing temperature shifts the cross-bridge population in favor of the M.ADP.P_i state in the putative prepowerstroke conformation. Because of decreased flexibility of myosin heads, narrowing lattice spacing as sarcomere length increases could facilitate attachment and hence become a key modulator of the active force level. Further studies on lattice spacing effects are in progress.

The authors thank Dr. Franklin Fuchs and Dr. Albert M. Gordon for helpful comments, Mr. Gary Melvin of the Intramural Research Program of the National Institute of Arthritis and Musculoskeletal and Skin Diseases, National Institutes of Health for expert technical assistance, and the technical staff of Beamline X27C at the National Synchrotron Light Source for technical help.

This research was in part supported by the Intramural Research Program of the National Institute of Arthritis and Musculoskeletal and Skin Diseases of the National Institutes of Health, and by an NIH grant to D.M. (HL 67071).

REFERENCES

1. Kensler, R. W. 2005. The mammalian cardiac muscle thick filament: crossbridge arrangement. *J. Struct. Biol.* 149:303–312.
2. Stein, L. A., and M. P. White. 1987. Biochemical kinetics of porcine cardiac subfragment-1. *Circ. Res.* 60:39–49.

3. Fuchs, F., and D. A. Martyn. 2005. Length-dependent Ca(2+) activation in cardiac muscle: some remaining questions. *J. Muscle Res. Cell Motil.* 26:199–212.

4. Konhilas, J. P., T. C. Irving, and P. P. De Tombe. 2002. Frank-Starling law of the heart and the cellular mechanisms of length-dependent activation. *Pflugers Arch.* 445:305–310.

5. Brenner, B., L. C. Yu, and J. M. Chalovich. 1991. Parallel inhibition of active force and relaxed fiber stiffness in skeletal muscle by caldesmon: implications for the pathway to force generation. *Proc. Natl. Acad. Sci. USA.* 88:5739–5743.

6. Martyn, D. A., B. B. Adhikari, M. Regnier, J. Gu, S. Xu, and L. C. Yu. 2004. Response of equatorial x-ray reflections and stiffness to altered sarcomere length and myofilament lattice spacing in relaxed skinned cardiac muscle. *Biophys. J.* 86:1002–1011.

7. Malinchik, S., S. Xu, and L. C. Yu. 1997. Temperature-induced structural changes in the myosin thick filament of skinned rabbit psoas muscle. *Biophys. J.* 73:2304–2312.

8. Xu, S., G. Offer, J. Gu, H. D. White, and L. C. Yu. 2003. Temperature and ligand dependence of conformation and helical order in myosin filaments. *Biochemistry.* 42:390–401.

9. Geeves, M. A., and K. C. Holmes. 1999. Structural mechanism of muscle contraction. *Annu. Rev. Biochem.* 68:687–728.

10. Xu, S., J. Gu, T. Rhodes, B. Belknap, G. Rosenbaum, G. Offer, H. White, and L. C. Yu. 1999. The M.ADP.P(i) state is required for helical order in the thick filaments of skeletal muscle. *Biophys. J.* 77:2665–2676.

11. Xu, S., J. Gu, G. Melvin, and L. C. Yu. 2002. Structural characterization of weakly attached cross-bridges in the A*M*ATP state in permeabilized rabbit psoas muscle. *Biophys. J.* 82:2111–2122.

12. Matsubara, I., and B. M. Millman. 1974. X-ray diffraction patterns from mammalian heart muscle. *J. Mol. Biol.* 82:527–536.

13. Xu, S., D. A. Martyn, and L. C. Yu. 2006. Effects of temperature and ionic strength on cardiac myofilament structure: the disorder-order transition of the thick filament. *Biophys. J.* 90:1253a (Abstr.).

14. Xu, S., S. Malinchik, D Gilroy, Th. Kraft, B. Brenner, and L. C. Yu. 1997. X-ray diffraction studies of cross-bridges weakly bound to actin in relaxed skinned fibers of rabbit psoas muscle. *Biophys. J.* 73:2292–2303.

15. Xu, S., M. Kress, and H. E. Huxley. 1987. X-ray diffraction studies of the structural state of crossbridges in skinned frog sartorius muscle at low ionic strength. *J. Muscle Res. Cell Motil.* 8:39–54.

16. White, H. D., B. Belknap, and M. R. Webb. 1997. Kinetics of nucleoside triphosphate cleavage and phosphate release steps by associated rabbit skeletal actomyosin, measured using a novel fluorescent probe for phosphate. *Biochemistry.* 36:11828–11836.

17. Kensler, R. W. 2002. Mammalian cardiac muscle thick filaments: their periodicity and interactions with actin. *Biophys. J.* 82:1497–1508.

18. Gordon, A. M., E. Homsher, and M. Regnier. 2000. Regulation of contraction in striated muscle. *Physiol. Rev.* 80:853–924.

19. Lehrer, S. S., and M. A. Geeves. 1998. The muscle thin filament as a classical cooperative/allosteric regulatory system. *J. Mol. Biol.* 277: 1081–1089.

20. Maytum, R., B. Westerdorf, K. Jaquet, and M. A. Geeves. 2003. Differential regulation of the actomyosin interaction by skeletal and cardiac troponin isoforms. *J. Biol. Chem.* 278:6696–6701.

21. Holmes, K. C., and M. A. Geeves. 2000. The structural basis of muscle contraction. *Philos. Trans. R. Soc. Lond. B Biol. Sci.* 355:419–431.

22. Houdusse, A., and H. L. Sweeney. 2001. Myosin motors: missing structures and hidden springs. *Curr. Opin. Struct. Biol.* 11:182–194.

23. Himmel, D. M., S. Gourinath, L. Reshetnikova, Y. Shen, A. G. Szent-Gyorgyi, and C. Cohen. 2002. Crystallographic findings on the internally uncoupled and near-rigor states of myosin: further insights into the mechanics of the motor. *Proc. Natl. Acad. Sci. USA.* 99:12645–12650.

24. Martyn, D. A., and L. Smith. 2005. The temperature dependence of length-dependent activation in cardiac muscle. *Biophys. J.* 88:120a (Abstr.).

25. Fujita, H., and M. Kawai. 2002. Temperature effect on isometric tension is mediated by regulatory proteins tropomyosin and troponin in bovine myocardium. *J. Physiol. (Lond.).* 539:267–276.

26. Chalovich, J. M. 1992. Actin mediated regulation of muscle contraction. *Pharmac.Therapeutics.* 55:95–148.

27. Levine, R. J., Z. Yang, N. D. Epstein, L. Fananapazir, J. T. Stull, and H. L. Sweeney. 1998. Structural and functional responses of mammalian thick filaments to alterations in myosin regulatory light chains. *J. Struct. Biol.* 122:149–161.

28. Yang, Z., J. T. Stull, R. J. Levine, and H. L. Sweeney. 1998. Changes in interfilament spacing mimic the effects of myosin regulatory light chain phosphorylation in rabbit psoas fibers. *J. Struct. Biol.* 122: 139–148.

29. Metzger, J. M., M. L. Greaser, and R. L. Moss. 1989. Variations in cross-bridge attachment rate and tension with phosphorylation of myosin in mammalian skinned skeletal muscle fibers. Implications for twitch potentiation in intact muscle. *J. Gen. Physiol.* 93: 855–883.

30. Sweeney, H. L., and J. T. Stull. 1990. Alteration of cross-bridge kinetics by myosin light chain phosphorylation in rabbit skeletal muscle: implications for regulation of actin-myosin interaction. *Proc. Natl. Acad. Sci. USA.* 87:414–418.

31. Sweeney, H. L., B. F. Bowman, and J. T. Stull. 1993. Myosin light chain phosphorylation in vertebrate striated muscle: regulation and function. *Am. J. Physiol.* 264:C1085–C1095.

32. Olsson, M. C., J. R. Patel, D. P. Fitzsimons, J. W. Walker, and R. L. Moss. 2004. Basal myosin light chain phosphorylation is a determinant of Ca2+ sensitivity of force and activation dependence of the kinetics of myocardial force development. *Am. J. Physiol. Heart Circ. Physiol.* 287:H2712–H2718.

33. Smith, S. H., and F. Fuchs. 2002. Length dependence of cardiac myofilament Ca(2+) sensitivity in the presence of substitute nucleoside triphosphates. *J. Mol. Cell. Cardiol.* 34:547–554.

34. Fuchs, F., and D. A. Martyn. 2005. Length-dependent Ca(2+) activation in cardiac muscle: some remaining questions. *J. Muscle Res. Cell Motil.* 26:199–212.